

PREPARED FOR SUBMISSION TO JHEP

UT-HET-075, KIAS-P12077, KU-PH-012, UT-12-39

Electroweak phase transition and Higgs boson couplings in the model based on supersymmetric strong dynamics

Shinya Kanemura,^a Eibun Senaha,^b Tetsuo Shindou^c and Toshifumi Yamada^d

^a*Department of Physics, University of Toyama*

3190 Gofuku, Toyama 930-8555, Japan

^b*School of Physics, KIAS*

85 Hoegiro, Dongdaemu-gu, Seoul 130-722, Korea

^c*Division of Liberal Arts, Kogakuin University*

1-24-2 Nishi-Shinjuku, Tokyo 163-8677, Japan

^d*Department of Physics, University of Tokyo*

7-3-1 Hongo, Tokyo 113-0033, Japan

E-mail: kanemu@sci.u-toyama.ac.jp, senaha@kias.re.kr,

shindou@cc.kogakuin.ac.jp,

toshifumi@hep-th.phys.s.u-tokyo.ac.jp

ABSTRACT: We discuss a strongly-coupled extended Higgs sector with the 126 GeV Higgs boson, which is a low-energy effective theory of the supersymmetric $SU(2)_H$ gauge theory that causes confinement. In this effective theory, we study the parameter region where electroweak phase transition is of strongly first order, as required for successful electroweak baryogenesis. In such a parameter region, the model has a Landau pole at the order of 10 TeV, which corresponds to the confinement scale of the $SU(2)_H$ gauge theory. We find that the large coupling constant which blows up at the Landau pole results in large non-decoupling loop effects on low-energy observables, such as the Higgs-photon-photon vertex and the triple Higgs boson vertex. As phenomenological consequences of electroweak baryogenesis in our model, the Higgs-to-diphoton branching ratio is about 20% smaller while the triple Higgs boson coupling is more than about 20% larger than the standard model predictions. Such deviations may be detectable in future collider experiments.

KEYWORDS: Electroweak Baryogenesis, Extended Higgs Models, SUSY Dynamics

Contents

1	Introduction	1
2	Model	3
2.1	Lagrangian	3
2.2	Mass Matrices	5
2.3	Coupling Constants	6
3	Electroweak Phase Transition	7
4	Low-energy Observables	9
4.1	Decay Branching Ratio of the Higgs Boson into Diphoton	9
4.2	Triple Higgs Boson Coupling	10
5	Phenomenological Consequences	11
6	Conclusions	15
A	One-loop finite temperature effective potential	15
A.1	Thermal masses	16

1 Introduction

Successful electroweak baryogenesis (EWBG) [1] relies on sufficient amount of CP violation and strongly first order electroweak phase transition (EWPT). In the standard model (SM), it turns out that the Kobayashi-Maskawa phase is far too small to generate sufficient baryon asymmetry [2], and the EWPT is a smooth crossover for a Higgs boson with the mass above 73 GeV [3]. Therefore, the SM must be extended. In general, extra CP-phases naturally enter into extended Higgs models. On the other hand, the condition on the EWPT is directly connected to the structure of the Higgs potential.

Many attempts to obtain feasible EWBG scenarios have been done in the extended models [4–6, 8–10, 31]. Among them, much attention has been paid to the minimal supersymmetric SM (MSSM) so far. As pointed out in refs. [11], however, the light scalar top scenario that is necessary for successful EWBG in MSSM is in tension with the current experimental data, especially the Higgs signal strength measurements at the LHC. Therefore, it is time to consider alternative models for successful EWBG in some detail, taking the recent LHC data into account.

Now that the Higgs boson mass is found to be 126 GeV, models that realize strongly first order phase transition due to a thermal cubic term generally require relatively large coupling constants in the Higgs sector. Such large coupling constants can blow up below the Planck scale with a Landau pole. In this case, the model must be replaced by a more fundamental theory at the Landau pole. Recently, an ultraviolet (UV) complete framework has been proposed for an extended Higgs sector incorporating such large coupling constants [12], which is based on the SUSY $SU(2)_H$ gauge theory with six doublets, T_1, \dots, T_6 ($N_f = 3$), and one singlet as a UV theory. This simple gauge structure was originally applied to the minimal supersymmetric fat Higgs model [13]. The gauge theory is strongly-coupled at an infrared scale. In ref. [12], the $SU(2)_H$ doublets T_1, \dots, T_6 are confined to give mesonic superfields [14], which are identified with the MSSM Higgs superfields and other exotic superfields in the extended Higgs sector. The Landau pole at which the coupling constants in the extended Higgs sector blow up is nothing but the confinement scale of the $SU(2)_H$ gauge theory. A striking feature of this framework is that the large coupling constants as well as the field content of the extended Higgs sector automatically result from the dynamics of the SUSY gauge theory. The Landau pole is determined to be of the order of 10 TeV from the requirement of strongly first order EWPT [9].

The low-energy effective theory of the model in ref. [12] contains four Higgs doublet, a pair of charged singlet and a pair of neutral singlet chiral superfields. In order to avoid flavor-changing neutral current, additional discrete Z_2 symmetry is imposed on the model, under which extra two doublets and all the singlets are odd. When the discrete symmetry is exact, the lightest Z_2 -odd particle can be another dark matter candidate other than the lightest supersymmetric particle as long as it is electrically neutral. Since this framework has the Landau pole around 10 TeV, it is unclear whether the naïve seesaw mechanism [15] for tiny neutrino masses with very heavy Majorana masses can be applied or not. A radiative generation mechanism for tiny neutrino masses with Z_2 -odd extra scalar doublets and Z_2 -odd TeV scale right handed neutrinos [16, 17] may be compatible with our framework. By developing the model in ref. [12], we may be able to build a fundamental UV complete model whose low-energy effective theory can explain baryogenesis, dark matter and tiny neutrino mass simultaneously below its confinement scale.

In general, loop effects due to a heavy particle becomes suppressed from low energy observables in the large mass limit by the decoupling theorem [18]. However, when the mass mainly comes from the vacuum expectation value (VEV), the decoupling theorem does not hold, and nonvanishing loop effect can appear. In particular, large non-decoupling effects can appear in the triple Higgs boson coupling [19] and the decay branching ratio of the Higgs boson to diphoton [20]. Since the enhancement of first order EWPT also comes from the non-decoupling effect, the strength of first

order EWPT and those low-energy observables are correlated.¹ In fact, significant deviations of those observables from the SM predictions are found in the two Higgs doublet model when EWPT is of strongly first order [5]. Also in SUSY extended Higgs models such as the “four Higgs doublets + two charged singlets model”, it is possible to realize strongly first order EWPT by large non-decoupling loop effects [9], and at the same time large non-decoupling effects contribute to low-energy observables [23]. Since these models contain a Landau pole, it is unclear how these models are related to physics at UV scales. In addition, the correlation between the strength of EWPT and low-energy observables has not been properly studied based on UV complete models.

In this paper, we discuss phenomenology of the extended Higgs model that emerges as a low-energy effective theory of the SUSY $SU(2)_H$ gauge theory with six doublets and one singlet, proposed in ref. [12]. First we evaluate the strength of EWPT and seek for parameter regions where strongly first order EWPT occurs, as is necessary for successful EWBG. We then calculate, in such parameter regions, the Higgs-to-diphoton branching ratio and the triple Higgs boson coupling, the former of which is measurable by 5% accuracy [24] and the latter of which by 20% accuracy [25] in future collider experiments. The relationship among the strength of EWPT and these two quantities is investigated.

This paper is organized as follows. In the next section, we give a detailed description of the extended Higgs model with large coupling constants that originates from the SUSY $SU(2)_H$ gauge theory. In Section 3, we evaluate the strength of EWPT. In Section 4, we summarize the calculation of the decay branching ratio of the Higgs boson into diphoton and the triple Higgs boson coupling. In Section 5, we take a benchmark mass spectrum, and discuss the correlation among the strength of EWPT, the Higgs-to-diphoton branching ratio and the triple Higgs boson coupling in our extended Higgs model. The final section is devoted to conclusions.

2 Model

2.1 Lagrangian

We consider a supersymmetric (SUSY) extended Higgs sector that emerges as a low-energy effective theory of the SUSY $SU(2)_H$ gauge theory with three pairs of doublets and one singlet, which has been proposed in ref. [12]. In this model, the mesonic superfields of the $SU(2)_H$ gauge theory are identified with the Higgs

¹ The correlation between the strength of first order EWPT and the triple Higgs boson coupling has been discussed in different models in ref. [21], and that between the strength of first order EWPT and the Higgs-to-diphoton branching ratio has been discussed in a different model in ref. [22].

Field	$SU(2)_L$	$U(1)_Y$	Z_2
H_u	2	+1/2	+
H_d	2	-1/2	+
Φ_u	2	+1/2	-
Φ_d	2	-1/2	-
Ω^+	1	+1	-
Ω^-	1	-1	-
ζ, η	1	0	-
n_Φ, n_Ω	1	0	+

Table 1. Properties of the fields in the Higgs sector under the SM gauge groups and the Z_2 parity.

doublets of the MSSM as well as the extra chiral superfields in the extended Higgs sector. We stress that the field content and the superpotential of the model are uniquely determined by the dynamics of the gauge theory.

The model contains two $SU(2)_L$ doublet, two charged singlet and four neutral singlet chiral superfields, in addition to the two Higgs doublets of the MSSM. The model has a Z_2 parity, under which the MSSM fields and two neutral singlets are even and the others are odd. This parity forbids the Yukawa couplings between the extra $SU(2)_L$ doublets and matter superfields so that dangerous flavor changing neutral current processes are suppressed. The field content of the Higgs sector is summarized in Table 1. The superpotential of the Higgs sector is given by

$$\begin{aligned}
W_{Higgs} = & -\mu(H_u H_d - n_\Phi n_\Omega) - \mu_\Phi \Phi_u \Phi_d - \mu_\Omega(\Omega^+ \Omega^- - \zeta \eta) \\
& + \hat{\lambda} \left\{ H_d \Phi_u \zeta + H_u \Phi_d \eta - H_u \Phi_u \Omega^- - H_d \Phi_d \Omega^+ + n_\Phi \Phi_u \Phi_d + n_\Omega(\Omega^+ \Omega^- - \zeta \eta) \right\} .
\end{aligned} \tag{2.1}$$

$\hat{\lambda}$ denotes a running coupling constant for the fields in the extended Higgs sector. As for the superfields n_Φ and n_Ω , their scalar components couple to the MSSM Higgs scalars at tree level. However these couplings do not contribute to the one-loop effective potential for the MSSM Higgs scalars. We therefore ignore n_Φ and n_Ω in the following discussion. The soft SUSY breaking terms are introduced as follows:

$$\begin{aligned}
\mathcal{L}_{soft} = & -m_{H_u}^2 H_u^\dagger H_u - m_{H_d}^2 H_d^\dagger H_d - m_{\Phi_u}^2 \Phi_u^\dagger \Phi_u - m_{\Phi_d}^2 \Phi_d^\dagger \Phi_d \\
& - m_{\Omega^+}^2 \Omega^{+\dagger} \Omega^+ - m_{\Omega^-}^2 \Omega^{-\dagger} \Omega^- - m_\zeta^2 \zeta^\dagger \zeta - m_\eta^2 \eta^\dagger \eta \\
& - B\mu H_u H_d - B\mu_\Phi \Phi_u \Phi_d - B\mu_\Omega(\Omega^+ \Omega^- - \zeta \eta) \\
& - A_\zeta H_d \Phi_u \zeta - A_\eta H_u \Phi_d \eta - A_{\Omega^-} H_u \Phi_u \Omega^- - A_{\Omega^+} H_d \Phi_d \Omega^+ .
\end{aligned} \tag{2.2}$$

2.2 Mass Matrices

We denote the VEV of H_u^0 by $v_u/\sqrt{2}$ and that of H_d^0 by $v_d/\sqrt{2}$. We hereafter denote the value of the running coupling constant, $\hat{\lambda}$, at the electroweak scale by $\lambda \equiv \hat{\lambda}(\mu_{EW})$.

The scalar and fermionic components of H_u and H_d have the same mass spectrum as MSSM at tree level. The fermionic components of the Z_2 -odd superfields have the following mass matrices at tree level:

$$\mathcal{L}_{\text{odd charginos}} = - (\tilde{\Phi}_u^+, \tilde{\Omega}^+) \begin{pmatrix} -\mu_\Phi & \lambda v_u/\sqrt{2} \\ -\lambda v_d/\sqrt{2} & -\mu_\Omega \end{pmatrix} \begin{pmatrix} \tilde{\Phi}_d^- \\ \tilde{\Omega}^- \end{pmatrix} \quad (2.3)$$

$$\mathcal{L}_{\text{odd neutralinos}} = -\frac{1}{2} (\tilde{\Phi}_u^0, \tilde{\Phi}_d^0, \tilde{\zeta}, \tilde{\eta}) \begin{pmatrix} 0 & \mu_\Phi & \lambda v_d/\sqrt{2} & 0 \\ \mu_\Phi & 0 & 0 & -\lambda v_u/\sqrt{2} \\ \lambda v_d/\sqrt{2} & 0 & 0 & \mu_\Omega \\ 0 & -\lambda v_u/\sqrt{2} & \mu_\Omega & 0 \end{pmatrix} \begin{pmatrix} \tilde{\Phi}_u^0 \\ \tilde{\Phi}_d^0 \\ \tilde{\zeta} \\ \tilde{\eta} \end{pmatrix} \quad (2.4)$$

The scalar components of the Z_2 -odd superfields have the following mass matrices at tree level:

$$\begin{aligned} \mathcal{L}_{\text{odd charged scalars}} = & - ((\Phi_u^+)^*, (\Omega^+)^*, \Phi_d^-, \Omega^-) \times \\ & \begin{pmatrix} \bar{m}_{\Phi_u}^2 + \lambda^2 \frac{v_u^2}{2} + D_{\Phi\pm} & \lambda \mu_\Phi^* \frac{v_d}{\sqrt{2}} - \lambda \frac{v_u}{\sqrt{2}} \mu_\Omega & B \mu_\Phi^* & \lambda \mu \frac{v_d}{\sqrt{2}} - A_{\Omega^-}^* \frac{v_u}{\sqrt{2}} \\ \lambda \mu_\Phi \frac{v_d}{\sqrt{2}} - \lambda \mu_\Omega^* \frac{v_u}{\sqrt{2}} & \bar{m}_{\Omega^+}^2 + \lambda^2 \frac{v_d^2}{2} + D_{\Omega\pm} & -\lambda \mu \frac{v_u}{\sqrt{2}} + A_{\Omega^+}^* \frac{v_d}{\sqrt{2}} & B \mu_\Omega^* \\ B \mu_\Phi & -\lambda \mu^* \frac{v_u}{\sqrt{2}} + A_{\Omega^+} \frac{v_d}{\sqrt{2}} & \bar{m}_{\Phi_d}^2 + \lambda^2 \frac{v_d^2}{2} - D_{\Phi\pm} & \lambda \mu_\Omega^* \frac{v_d}{\sqrt{2}} - \lambda \mu_\Phi \frac{v_u}{\sqrt{2}} \\ \lambda \mu^* \frac{v_d}{\sqrt{2}} - A_{\Omega^-}^* \frac{v_u}{\sqrt{2}} & B \mu_\Omega & \lambda \mu_\Omega \frac{v_d}{\sqrt{2}} - \lambda \mu_\Phi^* \frac{v_u}{\sqrt{2}} & \bar{m}_{\Omega^-}^2 + \lambda^2 \frac{v_u^2}{2} - D_{\Omega\pm} \end{pmatrix} \\ & \times \begin{pmatrix} \Phi_u^+ \\ \Omega^+ \\ (\Phi_d^-)^* \\ (\Omega^-)^* \end{pmatrix} \end{aligned} \quad (2.5)$$

$$\begin{aligned} \mathcal{L}_{\text{odd neutral scalars}} = & - ((\Phi_u^0)^*, \zeta, \Phi_d^0, (\eta)^*) \times \\ & \begin{pmatrix} \bar{m}_{\Phi_u}^2 + \lambda^2 \frac{v_d^2}{2} + D_{\Phi 0} & \lambda \mu \frac{v_u}{\sqrt{2}} + A_\zeta^* \frac{v_d}{\sqrt{2}} & B \mu_\Phi^* & \lambda \mu_\Omega \frac{v_d}{\sqrt{2}} - \lambda \mu_\Phi^* \frac{v_u}{\sqrt{2}} \\ \lambda \mu^* \frac{v_u}{\sqrt{2}} + A_\zeta \frac{v_d}{\sqrt{2}} & \bar{m}_\zeta^2 + \lambda^2 \frac{v_d^2}{2} & \lambda \mu_\Phi^* \frac{v_d}{\sqrt{2}} - \lambda \mu_\Omega \frac{v_u}{\sqrt{2}} & B \mu_\Omega \\ B \mu_\Phi & \lambda \mu_\Phi \frac{v_d}{\sqrt{2}} - \lambda \mu_\Omega^* \frac{v_u}{\sqrt{2}} & \bar{m}_{\Phi_d}^2 + \lambda^2 \frac{v_u^2}{2} - D_{\Phi 0} & -\lambda \mu^* \frac{v_d}{\sqrt{2}} - A_\eta \frac{v_u}{\sqrt{2}} \\ \lambda \mu_\Omega^* \frac{v_d}{\sqrt{2}} - \lambda \mu_\Phi \frac{v_u}{\sqrt{2}} & B \mu_\Omega^* & -\lambda \mu \frac{v_d}{\sqrt{2}} - A_\eta^* \frac{v_u}{\sqrt{2}} & \bar{m}_\eta^2 + \lambda^2 \frac{v_u^2}{2} \end{pmatrix} \\ & \times \begin{pmatrix} \Phi_u^0 \\ (\zeta)^* \\ (\Phi_d^0)^* \\ \eta \end{pmatrix} \end{aligned} \quad (2.6)$$

In eqs. (2.5) and (2.6), $\bar{m}_{\Phi_{u/d}}^2$, $\bar{m}_{\Omega^\pm}^2$, \bar{m}_ζ^2 and \bar{m}_η^2 are defined as

$$\begin{aligned}\bar{m}_{\Phi_{u/d}}^2 &\equiv |\mu_\Phi|^2 + m_{\Phi_{u/d}}^2, \\ \bar{m}_{\Omega^\pm}^2 &\equiv |\mu_\Omega|^2 + m_{\Omega^\pm}^2, \\ \bar{m}_\zeta^2 &\equiv |\mu_\Omega|^2 + m_\zeta^2, \\ \bar{m}_\eta^2 &\equiv |\mu_\Omega|^2 + m_\eta^2,\end{aligned}\tag{2.7}$$

and D_{Φ^\pm} , D_{Ω^\pm} and $D_{\Phi 0}$ represent D-term contributions that are given by

$$\begin{aligned}D_{\Phi^\pm} &= \frac{g_Y^2}{8} (v_u^2 - v_d^2) - \frac{g^2}{8} (v_u^2 - v_d^2), \\ D_{\Omega^\pm} &= \frac{g_Y^2}{2} (v_u^2 - v_d^2), \\ D_{\Phi 0} &= \frac{g_Y^2}{8} (v_u^2 - v_d^2) + \frac{g^2}{8} (v_u^2 - v_d^2),\end{aligned}\tag{2.8}$$

where g_Y and g respectively denote the gauge couplings of $U(1)_Y$ (normalized so that H_u has charge $Y = +1/2$) and $SU(2)_L$.

We define $m_{\Phi_1'0}^2$ and $m_{\Phi_1'^\pm}^2$ as the smallest eigenvalues of the Z_2 -odd neutral scalar mass matrix, eq. (2.5), and the Z_2 -odd neutral scalar mass matrix, eq. (2.6), respectively.

2.3 Coupling Constants

The superpotential, eq. (2.1), emerges as an effective theory below the confinement scale of the $SU(2)_H$ gauge theory. The running coupling constant, $\hat{\lambda}$, in the superpotential is estimated in the following way. At the confinement scale of the $SU(2)_H$ gauge theory, Λ_H , SUSY Naïve Dimensional Analysis [26] suggests

$$\hat{\lambda}(\Lambda_H) \simeq 4\pi.\tag{2.9}$$

Below Λ_H , $\hat{\lambda}$ obeys the following renormalization group equation:

$$\mu \frac{d\hat{\lambda}}{d\mu} \simeq \frac{6}{16\pi^2} \hat{\lambda}^3,\tag{2.10}$$

where we neglect the electroweak gauge couplings. Conversely, once we know the value of the coupling constant $\hat{\lambda}$ at the electroweak scale, we can determine the confinement scale Λ_H by using eqs. (2.9) and (2.10). Figure 1 describes the renormalization group running of $\hat{\lambda}$ for each value of $\hat{\lambda}$ at the electroweak scale, $\lambda \equiv \hat{\lambda}(\mu_{EW})$. For example, if $\lambda = 1.6$ ($\lambda = 1.8$), the confinement scale exists around 15 TeV (5 TeV). We note that the relation between the value of λ and the confinement scale Λ_H is rather robust even though the estimate eq. (2.9) is subject to $O(1)$ ambiguity,

because the running coupling constant $\hat{\lambda}(\mu)$ shows a steep rise near the confinement scale. We also note that, if the coupling constants at the scale Λ_H are not universal and differ by the factor of 2, those at the electroweak scale differ at most by the factor of 0.1. As an example, we show in Figure (2) the renormalization group running of the coupling constants for the case when the confinement scale is 5.3 TeV and the four coupling constants for the terms $H_d\Phi_u\zeta$, $H_u\Phi_d\eta$, $H_u\Phi_u\Omega^-$, $H_d\Phi_d\Omega^+$ in eq. (2.1) take the values of $1.4\times 4\pi$, $1.2\times 4\pi$, $0.8\times 4\pi$, $0.6\times 4\pi$ at that scale.

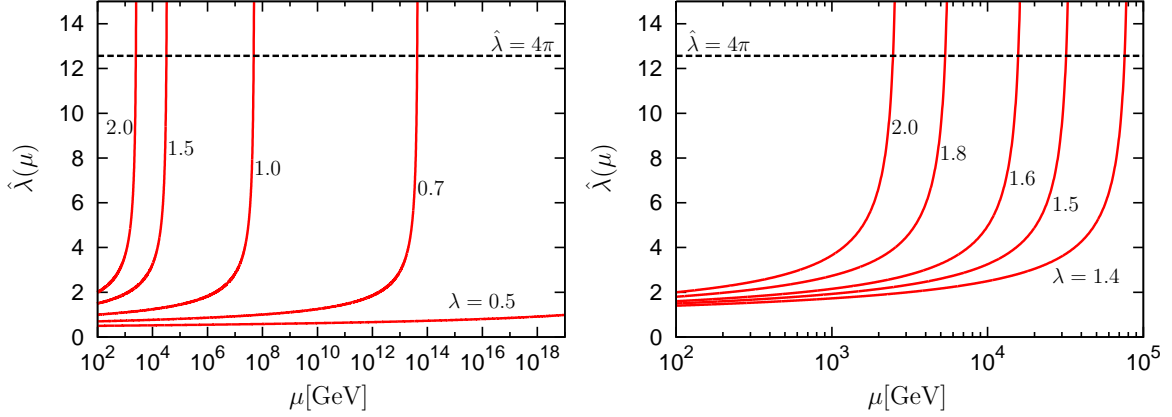


Figure 1. The renormalization group running of the coupling constant $\hat{\lambda}$ for each value of $\hat{\lambda}$ at the electroweak scale, $\lambda \equiv \hat{\lambda}(\mu_{EW})$.

3 Electroweak Phase Transition

In the EWBG scenario, the BAU is created in the symmetric phase where the $(B + L)$ -changing processes are active. In order to leave the generated BAU as it is, the $(B + L)$ -changing rate in the broken phase must be sufficiently suppressed. The conventional criterion is

$$\frac{v_c}{T_c} \gtrsim C, \quad (3.1)$$

where T_c denotes a critical temperature at which the effective potential has two degenerate minima, $v_c = \sqrt{v_d^2(T_c) + v_u^2(T_c)}$, and C is a parameter that depends on the sphaleron energy and so on. In this paper, we simply take $C \simeq 1$ rather than evaluating the precise value. In the MSSM, $C \simeq 1.4$ [31]. As demonstrated in ref. [9], v_c and T_c are determined using the one-loop effective potentials with ring resummations.

In the left panel of Figure 3, v_c and T_c are shown as a function of λ . We take $\tan \beta = 15$, $m_{H^\pm} = 350$ GeV, $\bar{m}_{\Omega^+}^2 = \bar{m}_{\Phi_d}^2 = \bar{m}_\zeta^2 = (1500 \text{ GeV})^2$, $\bar{m}_\eta^2 = (2000 \text{ GeV})^2$, $\bar{m}_{\Omega^-}^2 = \bar{m}_{\Phi_u}^2 = (50 \text{ GeV})^2$, $B_\Omega = B_\Phi = 0$ and $\mu_\Phi = -\mu_\Omega = 550$ GeV. We tune

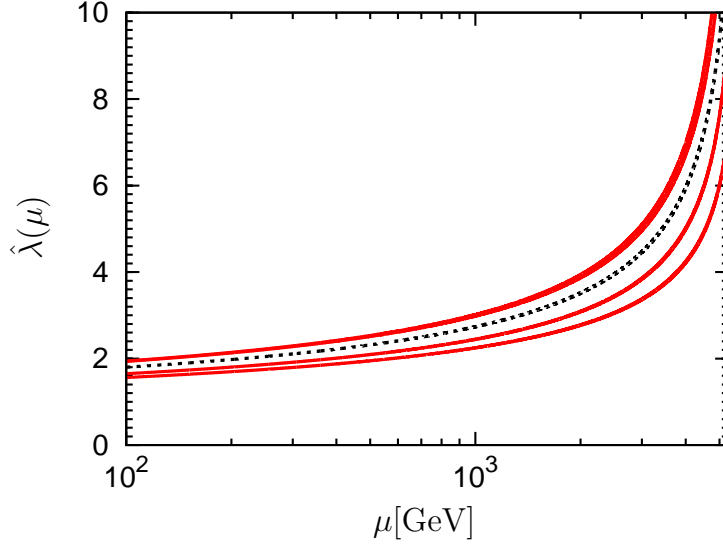


Figure 2. The renormalization group running of the coupling constants. The cut-off scale Λ_H is taken as $\Lambda_H = 5.3\text{GeV}$ which is relevant to $\lambda(\mu_{\text{EW}}) = 1.8$ in the universal coupling constant case. The dotted (black) line corresponds to the case with the universal coupling constant for the terms in the second line of eq. (2.1). The solide (red) lines are for the case (non-universal coupling constants case) when the first four terms in the second line of eq. (2.1) have different coupling constants at the cut-off scale Λ_H as $\hat{\lambda}(\Lambda_H) = 1.4 \times 4\pi, 1.2 \times 4\pi, 0.8 \times 4\pi, 0.6 \times 4\pi$.

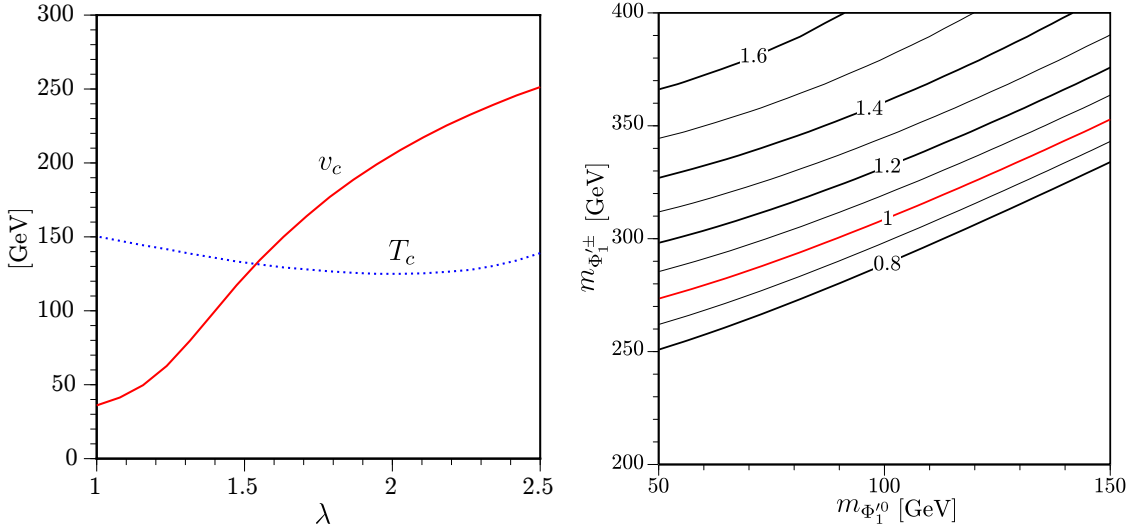


Figure 3. (Left panel) v_c and T_c as a function of λ . (Right panel) The contour of v_c/T_c in $m_{\Phi_1^\pm}$ - $m_{\Phi_1^0}$ plane. The input parameters are given in the text.

the A-term of the top squarks to realize 126 GeV mass for the SM-like Higgs boson. Similar to the results in ref. [9], $\lambda \gtrsim 1.6$ leads to $v_c/T_c \gtrsim 1$, which is due to the

nondecoupling effects arising from the Z_2 -odd charged Higgs boson loops. Note that the small $\bar{m}_{\Omega^-}^2$ and $\bar{m}_{\Phi_u}^2$ are necessary to realize such loop effects.

In the right panel of Figure 3, the contours of v_c/T_c are plotted. Here, $m_{\Phi_1^\pm}$ and $m_{\Phi_1^0}$ are treated as the input parameters, and $\bar{m}_{\Omega^-}^2$ and λ are derived quantities. The value of $m_{\Phi_1^0}$ more or less fixes $\bar{m}_{\Omega^-}^2$, and so the size of $m_{\Phi_1^\pm}$ is mostly controlled by λv_u . Therefore, the nondecoupling loop effects would be strengthened as $m_{\Phi_1^0}$ decreases and $m_{\Phi_1^\pm}$ increases. The plot clearly shows that v_c/T_c gets enhanced in such a nondecoupling region. This example indicates that $m_{\Phi_1^\pm} \gtrsim 270$ GeV with a relatively light Φ_1^0 are required to be consistent with successful electroweak baryogenesis.

4 Low-energy Observables

In this section, we summarize the methods to evaluate the two experimentally observable quantities, the branching ratio of the SM-like Higgs boson into diphoton and the triple Higgs boson coupling (at zero temperature), and their deviations from the SM predictions.

4.1 Decay Branching Ratio of the Higgs Boson into Diphoton

In our model, Z_2 -odd charged bosons and fermions alter the branching ratio of the SM-like Higgs boson into diphoton, $Br(h \rightarrow \gamma\gamma)$. Such effects can be significantly large because $h \rightarrow \gamma\gamma$ process arises only at loop levels, and the loop diagrams involving Z_2 -odd charged bosons and fermions are enhanced by their large coupling constant λ with MSSM Higgs superfields. The amplitude for the one-loop diagram involving the Z_2 -odd charged bosons is given by [27]

$$\mathcal{A}_S = C_0 \sum_{i=1,\dots,4} s_i \lambda^2 \frac{v^2}{\sqrt{2}m_{\phi_i^\pm}^2} \frac{1}{x_{\phi_i^\pm}^2} \{-x_{\phi_i^\pm} + f(x_{\phi_i^\pm})\}, \quad (4.1)$$

and that for the one-loop diagram involving the Z_2 -odd charged fermions is given by

$$\mathcal{A}_F = C_0 \sum_{j=1,2} f_j \lambda^2 \frac{v}{m_{\chi_j^\pm}} \frac{2}{x_{\chi_j^\pm}^2} \{x_{\chi_j^\pm} + (x_{\chi_j^\pm} - 1)f(x_{\chi_j^\pm})\}, \quad (4.2)$$

where C_0 is a common constant, $x_{\phi_i^\pm}$ and $x_{\chi_j^\pm}$ are respectively defined as

$$x_{\phi_i^\pm} \equiv m_h^2/4m_{\phi_i^\pm}^2, \quad x_{\chi_j^\pm} \equiv m_h^2/4m_{\chi_j^\pm}^2, \quad (4.3)$$

and the function $f(x)$ is defined as

$$f(x) \equiv \arcsin^2(\sqrt{x}) \quad (4.4)$$

for $x \leq 1$. Here ϕ_i^\pm ($i = 1, 2, 3, 4$) denote the four mass eigenstates of the Z_2 -odd charged scalars and χ_j^\pm ($j = 1, 2$) denote the two mass eigenstates of the Z_2 -odd charged fermions. The coefficients s_i denote the couplings between the charged scalars ϕ_i^\pm and the Higgs boson h normalized by $\lambda^2 v$, and f_j denote those between the charged fermions χ_j^\pm and h normalized by λ . We note that s_i and f_j depend on the mixings in the Higgs sector in a complicated way, but at least two of s_i 's and one of f_j 's are of order 1.

The contributions from one-loop diagrams involving the MSSM charged Higgs boson and charginos are negligible compared to those from Z_2 -odd fields because they are suppressed by the ratios of the electroweak gauge couplings over λ . The ratio of $Br(h \rightarrow \gamma\gamma)$ over its SM value, $\mu_{\gamma\gamma}$, is written as

$$\mu_{\gamma\gamma} \equiv \frac{Br(h \rightarrow \gamma\gamma)}{Br(h \rightarrow \gamma\gamma)|_{SM}} = \frac{|\mathcal{A}_t + \mathcal{A}_W + \mathcal{A}_S + \mathcal{A}_F|^2}{|\mathcal{A}_t + \mathcal{A}_W|^2}. \quad (4.5)$$

4.2 Triple Higgs Boson Coupling

Radiative corrections due to Z_2 -odd bosons and fermions affect the (zero temperature) triple Higgs boson coupling and causes its deviation from the SM value. The deviation can be drastically large because of the large coupling λ between Z_2 -odd superfields and MSSM Higgs superfields [23].

We evaluate the triple Higgs boson coupling by using the one-loop effective potential [28]. In our model, assuming that the Z_2 -parity is not spontaneously broken, the one-loop effective potential is given by

$$\begin{aligned} V_{1\text{-loop}}[h_u, h_d, a_u, a_d] = & \frac{1}{64\pi^2} \left\{ g_s \sum_{i=1}^4 m_{\phi_i^0}^4(h_u, h_d, a_u, a_d) \left[\log \frac{m_{\phi_i^0}^2(h_u, h_d, a_u, a_d)}{Q^2} - \frac{3}{2} \right] \right. \\ & + g_s \sum_{i=1}^4 m_{\phi_i^\pm}^4(h_u, h_d, a_u, a_d) \left[\log \frac{m_{\phi_i^\pm}^2(h_u, h_d, a_u, a_d)}{Q^2} - \frac{3}{2} \right] \\ & - g_M \sum_{i=1}^4 m_{\chi_i^0}^4(h_u, h_d, a_u, a_d) \left[\log \frac{m_{\chi_i^0}^2(h_u, h_d, a_u, a_d)}{Q^2} - \frac{3}{2} \right] \\ & \left. - g_D \sum_{i=1}^2 m_{\chi_i^\pm}^4(h_u, h_d, a_u, a_d) \left[\log \frac{m_{\chi_i^\pm}^2(h_u, h_d, a_u, a_d)}{Q^2} - \frac{3}{2} \right] \right\}, \end{aligned} \quad (4.6)$$

where Q corresponds to a renormalization scale, $m_{\phi_i^0}$, $m_{\phi_i^\pm}$, $m_{\chi_i^0}$ and $m_{\chi_i^\pm}$ respectively denote the mass eigenvalues of Z_2 -odd neutral scalars, charged scalars, neutral Majorana fermions and charged Dirac fermions which depend on the values of the

neutral components of the MSSM Higgs bosons,

$$\langle H_u^0 \rangle = \frac{h_u}{\sqrt{2}} + i \frac{a_u}{\sqrt{2}}, \quad \langle H_d^0 \rangle = \frac{h_d}{\sqrt{2}} + i \frac{a_d}{\sqrt{2}}, \quad (4.7)$$

and g_s , g_M and g_D respectively count the physical degrees of freedom of a complex scalar, a Majorana fermion and a Dirac fermion, and are given as $g_s = 2$, $g_M = 2$ and $g_D = 4$.

The Higgs potential at one-loop level is written as

$$V[h_u, h_d, a_u, a_d] = V_{\text{tree}} + V_{1\text{-loop}}, \quad (4.8)$$

where V_{tree} denotes the tree level potential. The mass eigenstates h , H and A as well as the Nambu-Goldstone mode G are related to h_u , h_d , a_u and a_d by

$$\begin{pmatrix} h_u \\ h_d \end{pmatrix} = \begin{pmatrix} \cos \alpha & \sin \alpha \\ -\sin \alpha & \cos \alpha \end{pmatrix} \begin{pmatrix} h \\ H \end{pmatrix}, \quad (4.9)$$

$$\begin{pmatrix} a_u \\ a_d \end{pmatrix} = \begin{pmatrix} \sin \beta & \cos \beta \\ -\cos \beta & \sin \beta \end{pmatrix} \begin{pmatrix} G \\ A \end{pmatrix}. \quad (4.10)$$

We here choose as a set of input parameters $v(\equiv \sqrt{v_u^2 + v_d^2} \simeq 246 \text{ GeV})$, $\tan \beta(\equiv v_u/v_d)$, m_h , m_H , m_A , where m_φ denotes the mass of φ , and the mixing angle of the CP-even Higgs bosons α . We impose the following renormalization conditions. At $h_u = v \sin \beta(= v_u)$, $h_d = v \cos \beta(= v_d)$ and $a_u = a_d = 0$,

$$\frac{\partial V}{\partial h} = \frac{\partial V}{\partial H} = 0, \quad (4.11)$$

$$\frac{\partial^2 V}{\partial h^2} = m_h^2, \quad \frac{\partial^2 V}{\partial H^2} = m_H^2, \quad \frac{\partial^2 V}{\partial H \partial h} = 0, \quad \frac{\partial^2 V}{\partial A^2} = m_A^2. \quad (4.12)$$

The one-loop corrected triple Higgs boson coupling, λ_{hhh} , is evaluated as

$$\lambda_{hhh} = \frac{\partial^3 V}{\partial h^3} [v_u, v_d, 0, 0]. \quad (4.13)$$

For convenience, we define “the deviation of the triple Higgs boson coupling from the SM value”, $\Delta\lambda_{hhh}/\lambda_{hhh}|_{SM}$, as

$$\frac{\Delta\lambda_{hhh}}{\lambda_{hhh}|_{SM}} \equiv \frac{\lambda_{hhh} - \lambda_{hhh}|_{SM}}{\lambda_{hhh}|_{SM}}. \quad (4.14)$$

5 Phenomenological Consequences

We make a numerical analysis on the correlation among the strength of EWPT, the decay branching ratio of the Higgs boson into diphoton and the triple Higgs boson

coupling, for a benchmark mass spectrum. The benchmark is as follows. For the MSSM sector,

$$\begin{aligned}\tan\beta &= 15, \quad m_{H^\pm} = 350 \text{ GeV}, \quad \mu = 200 \text{ GeV}, \\ \tilde{M}_{\tilde{t}} &= \tilde{M}_{\tilde{b}} = 2000 \text{ GeV}.\end{aligned}\tag{5.1}$$

For the Z_2 -odd sector,

$$\begin{aligned}\mu_\Phi &= \mu_\Omega = 550 \text{ GeV}, \\ \bar{m}_{\Phi_d} &= \bar{m}_{\Omega^+} = \bar{m}_\zeta = 1500 \text{ GeV}, \quad \bar{m}_\eta = 2000 \text{ GeV}, \\ (\text{Aterms}, \text{Bterms}) &= 0.\end{aligned}\tag{5.2}$$

The following two quantities are the free parameters in this analysis:

$$\lambda, \quad m_0 \left(\equiv \bar{m}_{\Phi_u} = \bar{m}_{\Omega^-} \right).\tag{5.3}$$

We tune the value of the stop mixing term to realize $m_h = 126 \text{ GeV}$.

The results are shown by contour plots on the plane of $m_{\Phi_1^0}$ and $m_{\Phi_1^\pm}$, defined respectively as the smallest eigenvalues of the Z_2 -odd neutral scalar mass matrix in eq. (2.5) and the Z_2 -odd neutral scalar mass matrix in eq. (2.6). Notice that $m_{\Phi_1^0}$ and $m_{\Phi_1^\pm}$ are in one-to-one correspondence with λ and m_0 in eq. (5.3). In Figure 4, we show the contour plot for the coupling constant λ . The strength of EWPT, $v_C/T_C = 1$, is also displayed. We find that strongly first order phase transition, $v_C/T_C \gtrsim 1$, takes places with our benchmark mass spectrum for $\lambda \gtrsim 1.6$ when $m_{\Phi_1^0} \simeq 60 \text{ GeV}$ (for $\lambda \gtrsim 1.8$ when $m_{\Phi_1^0} \simeq 130 \text{ GeV}$). Loop corrections involving light Z_2 -odd scalars strengthen the order of EWPT. Hence the lighter the lightest Z_2 -odd scalar is, the smaller value of λ we need to realize $v_C/T_C \gtrsim 1$. We also note that the value of λ corresponds to the confinement scale, Λ_H , of the SUSY $SU(2)_H$ gauge theory in UV. According to Figure 1, $\lambda \simeq 1.6$ corresponds to $\Lambda_H \simeq 15 \text{ TeV}$ and $\lambda \simeq 1.8$ does to $\Lambda_H \simeq 5 \text{ TeV}$.

In Figure 5, we combine the contour plot for the ratio of the Higgs-to-diphoton branching ratio over its SM value, $\mu_{\gamma\gamma}$, with a line indicating the strength of EWPT, $v_C/T_C = 1$. We find that the Higgs-to-diphoton branching ratio decreases by more than 20 % with our benchmark mass spectrum when the strongly first order phase transition with $v_C/T_C \gtrsim 1$ is realized. The deviation of the branching ratio, $\mu_{\gamma\gamma}$, exhibits only a mild dependence on $m_{\Phi_1^0}$ and $m_{\Phi_1^\pm}$. This is because, in the sample mass spectrum, the mass of the lightest Z_2 -odd charged scalar increases with λ , $m_{\Phi_1^\pm} \sim \lambda v_u$. Therefore, for loop diagrams contributing to the Higgs-to-diphoton decay, the increase in the coupling between the SM-like Higgs boson and the charged scalar is cancelled by the increase in the charged scalar mass, and thus the deviation of the Higgs-to-diphoton decay is not sensitive to λ .

Finally in Figure 6, we combine the contour plot for the deviation of the triple Higgs boson coupling from the SM value, $\Delta\lambda_{hhh}/\lambda_{hhh}|_{SM}$, with a line indicating the

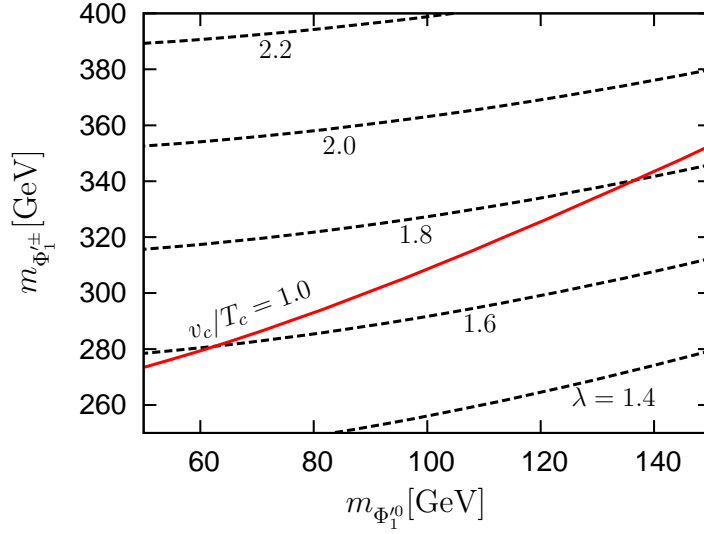


Figure 4. Contour plot for the coupling constant λ (black dashed lines) with a line corresponding to the strength of EWPT $v_C/T_C = 1$ (red solid line), on the plane of the mass of the lightest Z_2 -odd *charged* particle $m_{\Phi_1^\pm}$ and the mass of the lightest Z_2 -odd *neutral* particle $m_{\Phi_1^0}$. The parameters are fixed according to eqs. (5.1) and (5.2).

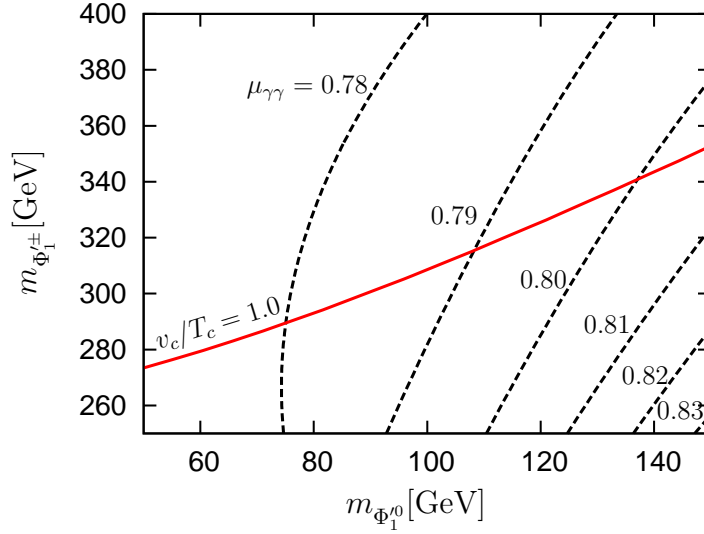


Figure 5. Contour plot for the ratio of $Br(h \rightarrow \gamma\gamma)$ over the SM value, $\mu_{\gamma\gamma}$ (black dashed lines), with a line corresponding to the strength of EWPT $v_C/T_C = 1$ (red solid line), on the plane of the mass of the lightest Z_2 -odd *charged* particle $m_{\Phi_1^\pm}$ and the mass of the lightest Z_2 -odd *neutral* particle $m_{\Phi_1^0}$. The parameters are fixed according to eqs. (5.1) and (5.2).

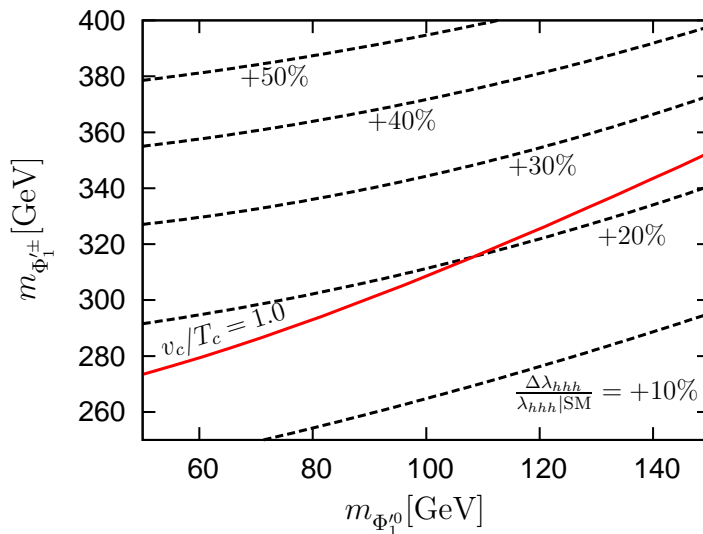


Figure 6. Contour plot for the deviation of the triple Higgs boson coupling from the SM value, $\Delta\lambda_{hhh}/\lambda_{hhh}|_{SM}$ (black dashed lines), with a line corresponding to the strength of EWPT $v_C/T_C = 1$ (red solid line), on the plane of the mass of the lightest Z_2 -odd *charged* particle $m_{\Phi_1^\pm}$ and the mass of the lightest Z_2 -odd *neutral* particle $m_{\Phi_1^0}$. The parameters are fixed according to eqs. (5.1) and (5.2).

strength of EWPT, $v_C/T_C = 1$. We discover that, when the strongly first order EWPT with $v_C/T_C \gtrsim 1$ occurs with our benchmark spectrum, the triple Higgs boson coupling increases by more than about 20 % for $150 \text{ GeV} > m_{\Phi_1^0} > 50 \text{ GeV}$. The strength of EWPT and the deviation of the triple Higgs boson coupling are correlated because the same loop corrections involving light Z_2 -odd scalars contribute to both of them.

To summarize, we confirm that sufficiently strong first order EWPT for successful EWBG can be realized with our benchmark mass spectrum. In order to have $v_C/T_C \gtrsim 1$, we need $\lambda > 1.6$ provided the lightest Z_2 -odd neutral scalar is heavier than 50 GeV. This corresponds to the confinement scale Λ_H lower than about 15 TeV. In the parameter regions where the strongly first order EWPT occurs, the Higgs-to-diphoton branching ratio, $Br(h \rightarrow \gamma\gamma)$, and the triple Higgs boson coupling, λ_{hhh} , significantly deviate from the SM values. These are principally due to loop corrections involving light Z_2 -odd scalars, which are also responsible for the strongly first order electroweak phase transition. With the benchmark mass spectrum, $Br(h \rightarrow \gamma\gamma)$ decreases by about 20% and λ_{hhh} increases by more than about 20%, both of which may be observed at the future International Linear Collider [24, 25] and its $\gamma\gamma$ option [29] and the Compact Linear Collider [30].

6 Conclusions

We have discussed the correlation among the strength of EWPT, the Higgs-to-diphoton branching ratio and the triple Higgs boson coupling in the extended Higgs sector with large coupling constants and the 126 GeV Higgs boson, which emerges as a low-energy effective theory of the SUSY $SU(2)_H$ gauge theory with confinement. In our benchmark mass spectrum, the condition of quick sphaleron decoupling for EWBG, $v_C/T_C \gtrsim 1$, determines the scale of the Landau pole to be below about 15 TeV, which corresponds to the confinement scale of the $SU(2)_H$ gauge theory. We have found that the Higgs-to-diphoton branching ratio deviates negatively from the SM prediction by about 20% and the triple Higgs boson coupling deviates positively by more than about 20%. Such deviations can be observed at future collider experiments.

Acknowledgments

This work was supported in part by Grant-in-Aid for Scientific Research, Nos. 22244031 (S.K.), 23104006 (S.K.), 23104011 (T.S.) and 24340046 (S.K. and T.S.). The work of T.Y. was supported in part by a grant of the Japan Society for the Promotion of Science, No. 23-3599.

A One-loop finite temperature effective potential

We study the electroweak phase transition in the subspace spanned by h_d and h_u , assuming the other fields do not develop the VEVs. The nonzero temperature effective potential is

$$V_1(h_d, h_u; T) = \sum_i c_i \frac{T^4}{2\pi^2} I_{B,F} \left(\frac{m_i^2}{T^2} \right), \quad (\text{A.1})$$

where c_i denote the degrees of freedom of the particle species i , $B(F)$ refer to boson (fermion) and $I_{B,F}$ take the form

$$I_{B,F}(a^2) = \int_0^\infty dx \, x^2 \ln \left(1 \mp e^{-\sqrt{x^2+a^2}} \right). \quad (\text{A.2})$$

For a reduction of a computational time, we use the fitting functions of $I_{B,F}(a^2)$ that are employed in Ref. [31]. More explicitly,

$$\tilde{I}_{B,F}(a^2) = e^{-a} \sum_{n=0}^N c_n^{b,f} a^n, \quad (\text{A.3})$$

are used, where $c_n^{b,f}$ are determined by the least square method. For $N = 40$, $|I_{B,F}(a^2) - \tilde{I}_{B,F}(a^2)| < 10^{-6}$ for any a , which is sufficient in our investigation.

As is well known, the validity of the perturbative expansion would get worse at high temperatures. The standard prescription for this problem is resummation of the dominant temperature corrections. Here, we adopt the Parwani's method [32] in which the both zero and nonzero modes of Matsubara frequencies are resummed. In this resummation scheme, the particle masses appearing in the one-loop effective potential are replaced with the thermally corrected masses.

A.1 Thermal masses

Let us define the temperature-dependent part of the self energy of a particle X by $\Sigma_X^{(Y)}(T)$, where Y denotes a particle in the loop. At the high temperature, $\Sigma_X^{(Y)}(T)$ can be expanded in powers of $m_Y/T (\equiv a_Y)$

$$\Sigma_X^{(Y)}(T) = C_{XY} \cdot I'_B(a_Y^2) \simeq C_{XY} \left[\frac{\pi^2}{12} - \frac{\pi}{4}(a_Y^2)^{1/2} - \frac{a_Y^2}{16} \left(\ln \frac{a_Y^2}{\alpha_B} - 1 \right) + \mathcal{O}(a_Y^4) \right], \quad (\text{A.4})$$

where C_{XY} denotes the coupling constant of X with Y and counts the degrees of freedom, $I'_B(a_Y^2)$ is the first derivative of $I_B(a_Y^2)$ with respect to a_Y^2 and $\ln \alpha_B = 2 \ln 4\pi - 2\gamma \simeq 3.9076$. The self energies of Ω^\pm , $\Phi_{u,d}$, ζ and η to leading order in the high temperature expansion are respectively given by

$$\begin{aligned} \Sigma_{\Omega^+}(T) &= \Sigma_{\Omega^+}^{(H_d)}(T) + \Sigma_{\Omega^+}^{(\Phi_d)}(T) + \Sigma_{\Omega^+}^{(\Omega^+)}(T) + \Sigma_{\Omega^+}^{(\Omega^-)}(T) \\ &= \left[\frac{|\lambda|^2}{6} + \frac{|\lambda|^2}{6} + \frac{g_Y^2}{6} - \frac{g_Y^2}{12} \right] T^2, \end{aligned} \quad (\text{A.5})$$

$$\begin{aligned} \Sigma_{\Omega^-}(T) &= \Sigma_{\Omega^-}^{(H_u)}(T) + \Sigma_{\Omega^-}^{(\Phi_u)}(T) + \Sigma_{\Omega^-}^{(\Omega^-)}(T) + \Sigma_{\Omega^-}^{(\Omega^+)}(T) \\ &= \left[\frac{|\lambda|^2}{6} + \frac{|\lambda|^2}{6} + \frac{g_Y^2}{6} - \frac{g_Y^2}{12} \right] T^2, \end{aligned} \quad (\text{A.6})$$

$$\begin{aligned} \Sigma_{\Phi_d}(T) &= \Sigma_{\Phi_d}^{(H_d)}(T) + \Sigma_{\Phi_d}^{(\Phi_d)}(T) + \Sigma_{\Phi_d}^{(\Phi_u)}(T) + \Sigma_{\Phi_d}^{(\eta)}(T) \\ &= \left[\frac{|\lambda|^2}{6} + \frac{g^2 + g_Y^2}{16} - \frac{g_Y^2}{24} + \frac{|\lambda|^2}{6} \right] T^2, \end{aligned} \quad (\text{A.7})$$

$$\begin{aligned} \Sigma_{\Phi_u}(T) &= \Sigma_{\Phi_u}^{(H_u)}(T) + \Sigma_{\Phi_u}^{(\Phi_u)}(T) + \Sigma_{\Phi_u}^{(\Phi_d)}(T) + \Sigma_{\Phi_u}^{(\zeta)}(T) \\ &= \left[\frac{|\lambda|^2}{6} + \frac{g^2 + g_Y^2}{16} - \frac{g_Y^2}{24} + \frac{|\lambda|^2}{6} \right] T^2, \end{aligned} \quad (\text{A.8})$$

$$\begin{aligned} \Sigma_\zeta(T) &= \Sigma_\zeta^{(H_d)}(T) + \Sigma_\zeta^{(\Phi_u)}(T) \\ &= \left[\frac{|\lambda|^2}{6} + \frac{|\lambda|^2}{6} \right] T^2, \end{aligned} \quad (\text{A.9})$$

$$\begin{aligned} \Sigma_\eta(T) &= \Sigma_\eta^{(H_u)}(T) + \Sigma_\eta^{(\Phi_d)}(T) \\ &= \left[\frac{|\lambda|^2}{6} + \frac{|\lambda|^2}{6} \right] T^2. \end{aligned} \quad (\text{A.10})$$

Here, we only show the Higgs boson loop contributions. The contributions of their superpartners are half of them.

Note that $I'_B(a^2)$ is Boltzmann suppressed for $a = m/T > 1$ as

$$I'_B(a^2) \simeq \frac{1}{2} \sqrt{\frac{\pi a}{2}} e^{-a} \left[1 + \frac{3}{8a} + \dots \right]. \quad (\text{A.11})$$

Therefore, we remove the T^2 corrections of $\Sigma_X^{(Y)}(T)$ from (A.5)-(A.10) in such a large mass region. In our analysis, in addition to the gauge bosons, Ω^- , Φ_u and H_u are potentially light enough to contribute to the screening effects since $\bar{m}_{\Omega^-} = \bar{m}_{\Phi_u} = 50$ GeV. It turns out that $|\bar{m}_{H_u}| > 200$ GeV in most parameter space. So the thermal resummation in our EWPT study are done by the following replacements ²

$$\bar{m}_{\Omega^-}^2 \rightarrow \bar{m}_{\Omega^-}^2 + \Sigma_{\Omega^-}^{(\Phi_u)}(T) + \Sigma_{\Omega^-}^{(\Omega^-)}(T) + \Sigma_{\Omega^-}^{(\text{gauge})}(T), \quad (\text{A.12})$$

$$\bar{m}_{\Phi_u}^2 \rightarrow \bar{m}_{\Phi_u}^2 + \Sigma_{\Phi_u}^{(\Phi_u)}(T) + \Sigma_{\Phi_u}^{(\text{gauge})}(T), \quad (\text{A.13})$$

where $\Sigma_{\Omega^-, \Phi_u}^{(\text{gauge})}(T)$ denote the gauge boson contributions.

References

- [1] V. A. Kuzmin, V. A. Rubakov and M. E. Shaposhnikov, Phys. Lett. B **155** (1985) 36. For reviews on the EWBG, see A. G. Cohen, D. B. Kaplan and A. E. Nelson, Ann. Rev. Nucl. Part. Sci. **43** (1993) 27; M. Quiros, Helv. Phys. Acta **67** (1994) 451; V. A. Rubakov and M. E. Shaposhnikov, Usp. Fiz. Nauk **166** (1996) 493; K. Funakubo, Prog. Theor. Phys. **96** (1996) 475; M. Trodden, Rev. Mod. Phys. **71** (1999) 1463; W. Bernreuther, Lect. Notes Phys. **591** (2002) 237; J. M. Cline, [arXiv:hep-ph/0609145]; D. E. Morrissey and M. J. Ramsey-Musolf, [arXiv:1206.2942 [hep-ph]].
- [2] M. B. Gavela, P. Hernandez, J. Orloff and O. Pene, Mod. Phys. Lett. A **9** (1994) 795; M. B. Gavela, P. Hernandez, J. Orloff, O. Pene and C. Quimbay, Nucl. Phys. B **430** (1994) 382; P. Huet and E. Sather, Phys. Rev. D **51** (1995) 379; T. Konstandin, T. Prokopec and M. G. Schmidt, Nucl. Phys. B **679** (2004) 246.
- [3] K. Kajantie, M. Laine, K. Rummukainen and M. E. Shaposhnikov, Phys. Rev. Lett. **77** (1996) 2887; K. Rummukainen, M. Tsypin, K. Kajantie, M. Laine and M. E. Shaposhnikov, Nucl. Phys. B **532** (1998) 283; F. Csikor, Z. Fodor and J. Heitger, Phys. Rev. Lett. **82** (1999) 21; Y. Aoki, F. Csikor, Z. Fodor and A. Ukawa, Phys. Rev. D **60** (1999) 013001.
- [4] M. Joyce, T. Prokopec and N. Turok, Phys. Rev. D **53** (1996) 2930; Phys. Rev. D **53** (1996) 2958; J. M. Cline, K. Kainulainen and A. P. Vischer, Phys. Rev. D **54** (1996)

²Even though the screening effect of H_u is taken into account, the critical line of $v_c/T_c = 1$ is not significantly changed. However, the maximal value of v_c/T_c cannot exceed 1.5 in this case.

- 2451; J. M. Cline and P. A. Lemieux, Phys. Rev. D **55** (1997) 3873; L. Fromme, S. J. Huber and M. Seniuch, JHEP **0611** (2006) 038; A. Kozhushko, V. Skalozub, Ukr. J. Phys. **56** (2011) 431-442; J. M. Cline, K. Kainulainen and M. Trott, JHEP **1111** (2011) 089 [arXiv:1107.3559 [hep-ph]]; T. Liu, M. J. Ramsey-Musolf and J. Shu, Phys. Rev. Lett. **108** (2012) 221301 [arXiv:1109.4145 [hep-ph]].
- [5] S. Kanemura, Y. Okada and E. Senaha, Phys. Lett. B **606** (2005) 361.
- [6] M. S. Carena, M. Quiros and C. E. M. Wagner, Phys. Lett. B **380** (1996) 81; D. Delepine, J. M. Gerard, R. Gonzalez Felipe and J. Weyers, Phys. Lett. B **386** (1996) 183; P. Huet and A. E. Nelson, Phys. Rev. D **53** (1996) 4578; B. de Carlos and J. R. Espinosa, Nucl. Phys. B **503** (1997) 24; M. S. Carena, M. Quiros, A. Riotto, I. Vilja and C. E. M. Wagner, Nucl. Phys. B **503** (1997) 387; M. Aoki, A. Sugamoto and N. Oshimo, Prog. Theor. Phys. **98** (1997) 1325; M. Aoki, N. Oshimo and A. Sugamoto, Prog. Theor. Phys. **98** (1997) 1179; J. M. Cline, M. Joyce and K. Kainulainen, JHEP **0007** (2000) 018; M. S. Carena, J. M. Moreno, M. Quiros, M. Seco and C. E. M. Wagner, Nucl. Phys. B **599** (2001) 158; M. S. Carena, M. Quiros, M. Seco and C. E. M. Wagner, Nucl. Phys. B **650** (2003) 24; C. Lee, V. Cirigliano and M. J. Ramsey-Musolf, Phys. Rev. D **71** (2005) 075010; V. Cirigliano, M. J. Ramsey-Musolf, S. Tulin and C. Lee, Phys. Rev. D **73** (2006) 115009; T. Konstandin, T. Prokopec, M. G. Schmidt and M. Seco, Nucl. Phys. B **738** (2006) 1; D. J. H. Chung, B. Garbrecht, M. J. Ramsey-Musolf and S. Tulin, Phys. Rev. Lett. **102** (2009) 061301; K. Funakubo, S. Tao and F. Toyoda, Prog. Theor. Phys. **109** (2003) 415; M. Carena, G. Nardini, M. Quiros and C. E. M. Wagner, Nucl. Phys. B **812** (2009) 243;
- [7] K. Funakubo and E. Senaha, Phys. Rev. D **79** (2009) 115024 [arXiv:0905.2022 [hep-ph]].
- [8] M. Pietroni, Nucl. Phys. B **402** (1993) 27; S. J. Huber and M. G. Schmidt, Nucl. Phys. B **606** (2001) 183; K. Funakubo, S. Tao and F. Toyoda, Prog. Theor. Phys. **114** (2005) 369; M. Carena, N. R. Shah and C. E. M. Wagner, Phys. Rev. D **85** (2012) 036003 [arXiv:1110.4378 [hep-ph]]; K. Cheung, T. -J. Hou, J. S. Lee and E. Senaha, Phys. Lett. B **710** (2012) 188 [arXiv:1201.3781 [hep-ph]].
- [9] S. Kanemura, E. Senaha and T. Shindou, Phys. Lett. B **706** (2011) 40.
- [10] R. Fok, G. D. Kribs, A. Martin and Y. Tsai [arXiv:1208.2784 [hep-ph]].
- [11] T. Cohen, D. E. Morrissey and A. Pierce, Phys. Rev. D **86** (2012) 013009; D. Curtin, P. Jaiswal and P. Meade, JHEP **1208** (2012) 005; M. Carena, G. Nardini, M. Quiros and C. E. M. Wagner, arXiv:1207.6330 [hep-ph].
- [12] S. Kanemura, T. Shindou and T. Yamada, Phys. Rev. D **86** (2012) 055023.
- [13] R. Harnik, G. D. Kribs, D. T. Larson and H. Murayama, Phys. Rev. D **70**, 015002 (2004) [hep-ph/0311349].
- [14] K. A. Intriligator and N. Seiberg, Nucl. Phys. Proc. Suppl. **45BC**, 1 (1996) [arXiv:hep-th/9509066].

- [15] P. Minkowski, Phys. Lett. B 67, 421 (1977); T. Yanagida, in Proceedings of the Workshop on the Unified Theory and the Baryon Number in the Universe (O. Sawada and A. Sugamoto, eds.), KEK, Tsukuba, Japan, 1979, p. 95; M. Gell-Mann, P. Ramond, and R. Slansky, Supergravity (P. van Nieuwenhuizen et al. eds.), North Holland, Amsterdam, 1979, p. 315; S. L. Glashow, The future of elementary particle physics, in Proceedings of the 1979 Cargèse Summer Institute on Quarks and Leptons (M. Levy et al. eds.), Plenum Press, New York, 1980, p. 687; R. N. Mohapatra and G. Senjanovic, Phys. Rev. Lett. 44, 912 (1980).
- [16] E. Ma, Phys. Rev. D 73, 077301 (2006) [hep-ph/0601225]; J. Kubo, E. Ma and D. Suematsu, Phys. Lett. B 642, 18 (2006) [hep-ph/0604114]; E. Ma, Annales Fond. Broglie 31, 285 (2006) [hep-ph/0607142]; H. Fukuoka, J. Kubo and D. Suematsu, Phys. Lett. B 678, 401 (2009) [arXiv:0905.2847 [hep-ph]]; E. Ma, Mod. Phys. Lett. A23, 721 (2008) [arXiv:0801.2545 [hep-ph]]; D. Suematsu and T. Toma, Nucl. Phys. B847, 567 (2011) [arXiv:1011.2839 [hep-ph]].
- [17] M. Aoki, S. Kanemura and O. Seto, Phys. Rev. Lett. 102, 051805 (2009) [arXiv:0807.0361 [hep-ph]]; M. Aoki, S. Kanemura and O. Seto, Phys. Rev. D80, 033007 (2009) [arXiv:0904.3829 [hep-ph]]; M. Aoki, S. Kanemura and K. Yagyu, Phys. Rev. D83, 075016 (2011) [arXiv:1102.3412 [hep-ph]].
- [18] T. Appelquist and J. Carazzone, Phys. Rev. D 11 (1975) 2856.
- [19] S. Kanemura, S. Kiyoura, Y. Okada, E. Senaha and C. P. Yuan, Phys. Lett. B 558 (2003) 157 [hep-ph/0211308]; S. Kanemura, Y. Okada, E. Senaha and C. -P. Yuan, Phys. Rev. D 70 (2004) 115002 [hep-ph/0408364].
- [20] I. F. Ginzburg, M. Krawczyk and P. Osland [arXiv:hep-ph/0211371].
- [21] A. Noble and M. Perelstein, Phys. Rev. D 78 (2008) 063518 [arXiv:0711.3018 [hep-ph]].
- [22] H. Davoudiasl, I. Lewis and E. Ponton, arXiv:1211.3449 [hep-ph].
- [23] S. Kanemura, T. Shindou and K. Yagyu, Phys. Lett. B 699 (2011) 258.
- [24] M. E. Peskin [arXiv:1207.2516 [hep-ph]].
- [25] A. Djouadi, W. Kilian, M. Muhlleitner and P. M. Zerwas, Eur. Phys. J. C 10 (1999) 27 [hep-ph/9903229]; K. Fujii, talk given at LCWS12, “Higgs Physics at the LC and Requirements” <http://www.uta.edu/physics/lcws12/>
- [26] H. Georgi, A. Manohar and G. W. Moore, Phys. Lett. B 149 (1984) 234; H. Georgi and L. Randall, Nucl. Phys. B 276 (1986) 241; M. A. Luty, Phys. Rev. D 57 (1998) 1531 [arXiv:hep-ph/9706235]; A. G. Cohen, D. B. Kaplan and A. E. Nelson, Phys. Lett. B 412 (1997) 301 [arXiv:hep-ph/9706275].
- [27] M. A. Shifman, A. Vainshtein, M. Voloshin and V. I. Zakharov, Sov. J. Nucl. Phys. 30 (1979) 711; G. K. S. D. John, F. Gunion and H. E. Haber, “The Higgs Hunters Guide” (Westview Press).
- [28] S. R. Coleman and E. J. Weinberg, Phys. Rev. D7 (1973) 1888.

- [29] S. Kawada *et al.* [arXiv:1205.5292 [hep-ph]].
- [30] D. Dannheim *et al.* [arXiv:1208.1402 [hep-ex]].
- [31] K. Funakubo and E. Senaha, Phys. Rev. D **79** (2009) 115024 [arXiv:0905.2022 [hep-ph]].
- [32] R. R. Parwani, Phys. Rev. D **45** (1992) 4695 [Erratum-ibid. D **48** (1993) 5965] [hep-ph/9204216].